Front. Struct. Civ. Eng. 2020, 14(3): 569–585
https://doi.org/10.1007/s11709-020-0607-6

RESEARCH ARTICLE

State-of-the-art on resistance of bearing-type bolted connections in high strength steel

Guoqiang LI[a], Yifan LYU[b], Yanbo WANG[b*]

[a] *State Key Laboratory for Disaster Reduction in Civil Engineering, Tongji University, Shanghai 200092, China*

[b] *College of Civil Engineering, Tongji University, Shanghai 200092, China*

[*] *Corresponding author. E-mail: ybwang@tongji.edu.cn*

ABSTRACT With the recent development of material science, high strength steel (HSS) has become a practical solution for landmark buildings and major projects. The current codes for design of bearing-type bolted connections of steel constructions were established based on the research of conventional steels. Since the mechanical properties of HSS are different from those of conventional steels, more works should be done to develop the appropriate approach for the design of bearing-type bolted connections in HSS. A review of the research carried out on bearing-type bolted connections fabricated from conventional steel and HSS is presented. The up-to-date tests conducted at Tongji University on four connection types fabricated from three grades of HSS with nominal yield strengths of 550, 690, and 890 MPa are presented. The previous research on failure modes, bearing resistance and the design with consideration of bolt hole elongation are summarized. It is found that the behavior of bolted connections in HSS have no drastic difference compared to that of conventional steel connections. Although the ductility is reduced, plastic deformation capacity of HSS is sufficient to ensure the load redistribution between different bolts with normal construction tolerances. It is also found that behavior of each bolt of multi-bolt connections arranged in perpendicular to load direction is almost identical to that of a single-bolt connection with the same end distance. For connections with bolts arranged in parallel to load direction, the deformation capacity of the whole connection depends on the minimum value between the end distance and the spacing distances in load direction. The comparison with existing design codes shows that Eurocode3 and Chinese GB50017-2017 are conservative for the design of bolted connections in HSS while AISC 360-16 may overestimate the bearing resistance of bolted connections.

KEYWORDS High strength steel, bolted connection, bearing behavior, design codes

1 Introduction

With development of material science, high strength steel (HSS) has provided a practical solution for the design of high-rise buildings. Generally, steel with a nominal yield strength equal to or over 460 MPa is defined as HSS [1–3]. Accordingly, steel with a nominal yield strength lower than 460 MPa is defined as conventional steel. Based on the process of Quenching and Tempering (Q + T) [4] or Thermo Mechanical Control Process (TMCP) [4], HSS has higher material strength than the conventional steel. The increase in material strength can effectively reduce the sectional size and self-weight of structural members. HSSs have been used in several landmark buildings, including NTV Tower in Japan (yield stress 600 MPa), Sony center in Germany (yield stress 460/690 MPa), and Millau Bridge in France (yield stress 460 MPa). Both economic benefits and improved structural efficiency can be achieved in these major projects due to the application of HSSs.

Bearing-type connection is a commonly used connection type at the construction site of steel structures. In bearing-type connection, the load is primarily transferred by bearing between the bolt shank and the hole wall of steel plate. If bolts are designed strong enough to avoid bolt shear failure, the ultimate resistance of connection is mainly determined by the steel plate. For connections designed with HSS plates, higher resistance of the whole connection is easily foreseen compared to those designed

Article history: Received Jul 30, 2018; Accepted Apr 29, 2019

with conventional steel. This is the most promising potential for application of HSS in the bearing-type bolted connection.

In bearing-type bolted connections, the development of resistance is accompanied with stress concentration around the bolt hole and significant plastic deformation. The favorable ductility of the conventional steel is sufficient for the plastic deformation around the bolt hole, which eases the effect of stress concentration. However, the ductility of steel is expected to decrease with the increase in material strength, which may affect the local deformation around bolts and the load redistribution among bolts. Splice connection with different number of bolts is a frequently used connection type to test the bearing resistance of bolted connections. Due to the simple experimental set-up and efficiency in acquiring the resistance of bearing-type connection, the tension splice has been mostly chosen in previous research references. According to the number of bolts, typical types of bolted connection specimens and conventions of the related geometric parameters are summarized in Fig. 1.

Connections fabricated from different grades of steel were tested in previous research references. According to the measured yield stress denoted as f_y, the steels are further classified into three categories as conventional steel ($f_y < 460$ MPa), HSS (460 MPa$\leqslant f_y < 1000$ MPa), and ultra-high strength steel ($f_y \geqslant 1000$ MPa). In total, 486 specimens from publications and 48 specimens tested at Tongji University are summarized in Table 1. The 48 connections tested by the authors at Tongji University were fabricated from HSSs with nominal yield strengths of 550, 690, and 890 MPa made in China. The proportion of the three categories of steels based on the collected specimens is shown in Table 1. It is found that 57% of tested specimens were fabricated from the conventional steels. HSS specimens take approximate 38% and the remaining 5% are ultra-high strength steel specimens.

The use of HSSs has been allowed in current codes, including Eurocode3 [26], American code AISC 360-16 [27], and Chinese code GB50017-2017 [28]. The allowed highest nominal yielding strength of steel specified in the Eurocode3, AISC 360-16, and GB50017-2017 are 700, 690, and 460 MPa, respectively. However, formulae of the bearing resistance of bolted connections in these three codes are based on the experimental results of conventional steels, as shown in Table 2. Clear mismatch between the specified steel grade and the tested steel grade is observed for all the three codes. Thus, it is necessary to check whether the current specifications are still applicable for bolted connections in HSSs.

This paper presents a state-of-the-art review on bearing-type bolted connections in HSSs. Previous research and recent test results of bearing-type bolted connections in three grades of HSSs conducted at Tongji University are summarized. The suitability of current Eurocode3, AISC 360-16, and GB50017-2017 for predicting the bearing resistance of bolted connections in HSSs are evaluated and discussed.

2 Single-bolt connection

2.1 Previous findings

The typical failure mode of the single-bolt connection observed by Kim and Yura [12] is shown in Fig. 2.

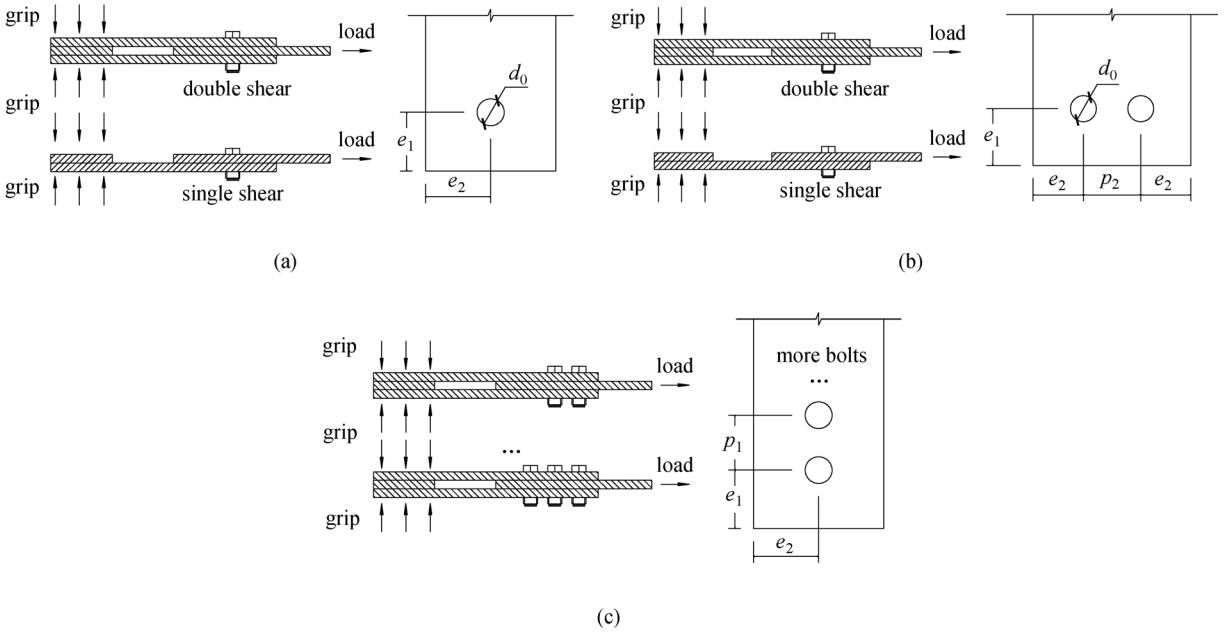

Fig. 1 Types of bolted connections for tests. (a) Type A: single-bolt connection; (b) Type B: two-bolt connection in parallel; (c) Type C: two-bolt or multi-bolt connection in tandem.

Table 1 Collected specimens in the previous specimens

source	connection types*	number of bolts	number of tested specimens according to f_y (MPa)		
			<460	$\geqslant 460$ and <1000	$\geqslant 1000$
Frank and Yura [5]	C	1, 2	30	0	0
Snijder et al. [6–8], Owens et al. [9–11]	A	1	111	23	0
Kim and Yura [12]	A, C	1,2	9	10	0
Puthli and Fleischer [13]	B	2	0	25	0
Aalberg and Larsen [14,15]	A, C	1,2	20	10	10
Clinton and Rex [16]	A	1	43	5	0
Može and Beg [17–19], Može [20]	A, B, C	1, 3, 4	47	59	0
Draganić et al. [21]	A, C	1	18	0	0
Guo et al. [22]	B, C	2	0	10	0
Shi et al. [23]	B	2	0	9	0
Liu et al. [24]	A, C	1, 2	7	0	0
Wu et al. [25]	A	1	20	20	0
the authors	A, B, C	1, 2, 3	0	32	16
sum			305	203	26
in total				534	
proportion			57%	38%	5%

*Note: Connection types are shown in Fig. 1.

Table 2 Allowed highest yield strength in current codes (MPa)

codes	allowed highest yield strength	yielding strength of tested specimens
Eurocode3	700	252–470
AISC 360-16	690	279–331
GB50017-2017	460	<370

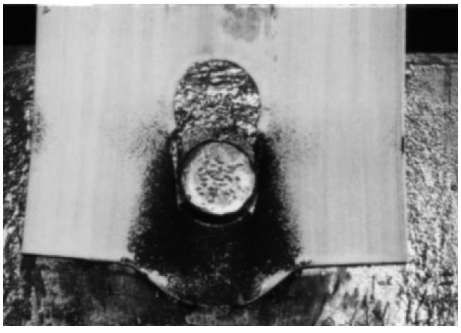

Fig. 2 Failure mode observed by Kim and Yura [12]. (Reprinted from Journal of Constructional Steel Research, 49(3), Kim H J & Yura J A, The effect of ultimate-to-yield ratio on the bearing strength of bolted connections, 255–269, Copyright 1999, with permission from Elsevier.)

Although two grades of steel with ultimate-to-yield stress ratio of 1.61 and 1.13 were used, the observed failure mode showed negligible difference. Kim and Yura [12] found that specimens with a low ultimate-to-yield stress ratio had a similar deformation capacity compared to those with a high ultimate-to-yield stress ratio, which was contrary to their initial expectation. They observed that tested specimens with larger end distance e_1 (defined in Fig. 1(a), e_1: end distance, from center of bolt hole to edge of plate parallel to load direction) had significantly increased deformation capacities. They concluded that end distance e_1 was a more significant factor on the deformation capacities than the ultimate-to-yield stress ratio. The result showed that the normalized resistances by $f_u dt$ (f_u is material ultimate stress, d is bolt diameter, t is plate thickness) recorded at 6.35 mm displacement have no obvious difference for specimens fabricated from different grades of steel with the ultimate-to-yield stress ratio greater than 1.13.

Snijder et al. [6–8] proposed a design formula for bearing-type connection based on the analysis of the behavior of single-bolt connection, which is the important support for formulae in current Eurocode3. Two ultimate limit states shown in Fig. 3 are defined. The first state is failure mode of plate shear, which mainly has two forms shown in Figs. 3(a) and 3(b), respectively. The second is excessive bolt hole elongation. Snijder et al. [6–8] considered that it was necessary to consider the bolt hole elongation, although the bolt hole elongation was not an ultimate limit state in the strict sense. To limit bolt hole elongation, Eq. (1) was established. The term $3f_y$ (f_y is material yield stress) was the mean ultimate bearing stress found by Snijder et al. [6–8]. For failure mode of plate shear, a simplified mode in Fig. 4 was used to derive

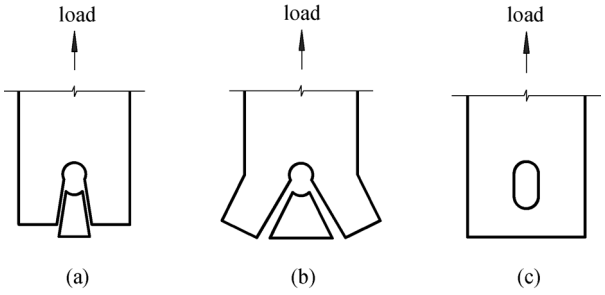

Fig. 3 Two ultimate limit states. (a) Plate shear mode of failure; (b) plate shear mode of failure; (c) bolt hole elongation.

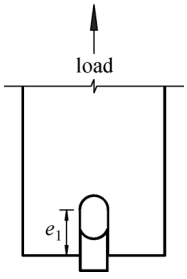

Fig. 4 Simplified failure mode of plate shear.

resistance. Assuming that the length of longitudinal shear planes in Fig. 4 is 0.9 times end distance e_1 and the shear stress is $0.6f_y$ according to von Mises yield criterion, Eq. (2) was established. With appropriate transformation, Eq. (3) replaced Eq. (2), where α approximately equals e_1/d_0 (d_0 is bolt hole diameter). To incorporate the consideration of bolt hole elongation, α should be lower than 3. As a result, a new parameter $\alpha' = \alpha/3$ was used to form a new formula in Eq. (4). A factor $\gamma_M = 1.25$ was further considered, which transforms the Eq. (4) to (5). To replace the yield stress f_y with the tensile stress f_u, the relationship between f_u and f_y in Eq. (6) was introduced. As a result, the final formula Eq. (7) was established for the design of bearing resistance, where $\alpha' = e_1/3d_0 \leqslant 1$. For multi-bolt connection, the parameter α' adopts $(p_1/3d_0 - 1/4) \leqslant 1$. Equation (7) is the original form for the design formulae in current Eurocode3.

For single-bolt connection (shown in Fig. 1(a)), the design bearing resistance is specified as Eq. (8) in current Eurocode3 while at the same time, washers should be set under both the head and nut. However, Kim and Yura [12] found that the actual bearing resistance could exceed the $1.5f_u dt$ by up to 42% in the tests. The limitation in the Eq. (8) may not reveal the actual bearing resistance.

$$F_{bs} = 3f_y dt, \tag{1}$$

where F_{bs} is bearing resistance, d is bolt diameter, and t is plate thickness, f_y is yield stress.

$$F_{bs} = 2 \times 0.9e_1 \times t \times 0.6f_y, \tag{2}$$

$$F_{bs} = \alpha f_y dt, \tag{3}$$

$$F_{bs} = 3\alpha' f_y dt, \tag{4}$$

$$F_{bs} = \frac{3.75\alpha' f_y dt}{\gamma_M}, \tag{5}$$

$$f_u = 1.5f_y, \tag{6}$$

$$F_{bs} = \frac{2.5\alpha' f_u dt}{\gamma_M}, \tag{7}$$

$$F_{bs} \leqslant \frac{1.5f_u dt}{\gamma_M}. \tag{8}$$

Two typical failure modes of the single-bolt connection were observed by Aalberg and Larsen [14,15]. They found that the first failure mode showed a close agreement with experiments reported by Kim and Yura [12]. The highest steel grade used by Aalberg and Larsen had a yield strength of 1340 MPa. For such ultra-high strength steel, significant bolt hole deformation could still be observed during the test. The final failure was a visible shear crack along the load direction. The second failure mode had a different feature compared to the first one. In addition to the shear crack, a tensile crack was found at the end edge of the specimen. The reason for this tensile crack is due to the transverse tensile stress at the edge caused by the splitting action of the bolt. For the deformation capabilities, no difference between the conventional steel (f_y = 388 MPa) and the HSS (f_y = 830 MPa) was observed. For the ultra-high strength steel (f_y = 1340 MPa), approximate 20% reduction of the deformation at fracture was observed compared to the other two steels. Similar to the conclusion by Kim and Yura [12], Aalberg and Larsen [14,15] concluded that end distance e_1 was a more significant effect on the deformation capacities of the connection than the steel grade. Comparison with Eurocode3 for the resistance of bearing-type connection was conducted by Aalberg and Larsen [14,15], which showed that predicted resistance of Eurocode3 was 76%, 85%, and 86% of the experimental ultimate resistance for the three steels, respectively. To achieve the same safety margin for connections in HSS, Aalberg and Larsen [14,15] suggested an additional strength reduction factor of 0.9 to Eurocode3. The test results from Aalberg and Larsen [14,15] indicated that some specimens did not possess the deformation capability of 6.35 mm at ultimate load. A theoretical background for the deformation of 6.35 mm was suggested in future research.

The investigations by Može and Beg [17,19] and Može [20] incorporated the edge distance e_2 (defined in Fig. 1(a), e_2: edge distance, from center of bolt hole to edge of plate perpendicular to load direction) into the experimental

parameters. Three typical failure modes were observed with varying edge distance e_2, as shown in Fig. 5. The change of failure mode related to the decreasing of edge distance e_2 was found. The first failure mode in Fig. 5(a) occurred when edge distance e_2 was wide enough to avoid net cross-section failure. Može and Beg [17] defined this failure mode as plate shear due to the shear fracture observed in the final failure mode. The second failure mode in Fig. 5(b) was referred as splitting failure. They found that the splitting failure was controlled by the net cross-section check and suggested to supplement the check for splitting failure in future designs. The third failure mode was net cross-section failure. It was found that behavior of the connection in net cross-section failure was ductile when gross-to-net cross-section ration is lower than the ultimate-to-yield stress ratio. Otherwise, non-ductile behavior of the connection occurred in the experiments. The comparison with Eurocode3 showed that Eurocode3 was conservative. They concluded that the resistance formula in Eurocode3 did not correlate to the actual bearing behavior of HSS plates. A new resistance formula shown in Eq. (9a) was proposed by Može and Beg [19]. The new formula has a linear relationship with the end distance e_1 while the effect of edge distance e_2 on the resistance is ignored. A strength reduction of 0.9 was applied to HSS, which was consistent with the suggestion by Aalberg and Larsen [14,15]. Equation (9a) was adopted in the research by Latour and Rizzano et al. [29] and achieved acceptable accuracy on the calculation of bearing resistance in tubular structures.

$$F_{bs} = k_b \alpha_d f_u dt, \tag{9a}$$

$$k_b = 1.0 \text{ for S235}, \ k_b = 0.9 \text{ for S690}, \tag{9b}$$

$$\alpha_d = e_1/d_0 \text{ for end bolt},$$

$$\alpha_d = p_1/d_0 - 0.75 \text{ for inner bolt}. \tag{9c}$$

Teh and Uz [30,31] studied the bearing behavior of single-bolt connections based on cold-reduced steel sheets. They found that different levels of snug-tightening would not cause significant variation in the bearing capacity of most bolted connections. A more important finding was that the absolute bearing capacity could be considerably lower in the direction perpendicular to the rolling direction of the steel sheet, even though the tensile strength is correspondingly higher. Thus, the future investigation on the effect of loading direction was suggested. Two failure modes as bearing and tearout failure defined in current AISC 360-16 are used by Teh and Uz [30], which are shown in Fig. 6. Equations (10) and (11) were suggested to predict the ultimate shear-out resistance and bearing resistance. The evaluation of ultimate shear-out resistance was based on active shear plane theory proposed by Teh and Uz [31]. Both Eqs. (10) and (11) achieved more consistent and accurate prediction than the current AISC 360-16 [27].

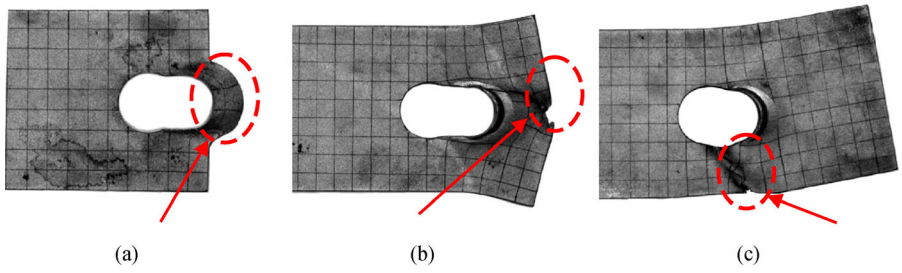

Fig. 5 Failure modes by Može and Beg [17]. (a) Tearout failure; (b) splitting failure; (c) net cross-section failure. (Reprinted from Journal of Constructional Steel Research, 66(8–9), Može P, Beg D, High strength steel tension splices with one or two bolts, 1000–1010, Copyright 2010, with permission from Elsevier.)

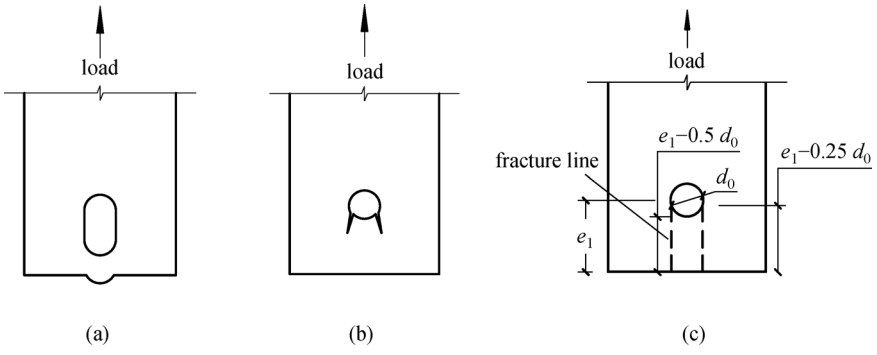

Fig. 6 Two failure modes and geometric parameter. (a) Bearing; (b) tearout; (c) geometry.

$$\text{tearout} \quad F_{bs} = 1.2(e_1 - 0.25d_0)f_u t, \tag{10}$$

$$\text{bearing} \quad F_{bs} = 3.5 f_u d t. \tag{11}$$

2.2 Test results and findings at Tongji University

Fifteen single-bolt connections (see Fig. 1(a)) with 3 grades of HSSs as Q550D, Q690D, Q890D were tested at Tongji University [32,33]. In accordance with GB/T 228-2002 [34], the measured material properties are reproduced in Table 3, where f_y is yield strength, f_u is tensile strength, E is elasticity modulus, ε_u is the strain at tensile strength, Δ is the elongation ratio at fracture. Five values of e_1 including e_1 = $1.0d_0$, $1.2d_0$, $1.5d_0$, $2.0d_0$, and $2.5d_0$ are designed, where d_0 is bolt hole diameter. To avoid net cross-section failure, the value of e_2 is fixed as $3.0d_0$ for all single-bolt connections. The connections are in double shear with grade 12.9 bolt to avoid bolt shear failure. The convention of specimens for single-bolt connection is SD-e_1/d_0-e_2/d_0-steel grade.

Table 3 Material property

steel grade	f_y (MPa)	f_u (MPa)	f_y/f_u	E (GPa)	ε_u	Δ (%)
Q550D	677	757	0.894	205	0.0642	18.5
Q690D	825	859	0.960	203	0.0511	13.5
Q890D	1022	1064	0.960	203	0.0590	14.5

The main observations and findings are summarized as follows.

1) Similar failure mode can be found for specimens with varying geometries and steel grades, which is shown in Fig. 7. No premature failure on the net cross-section is found. The final failure is a locally distributed shear fracture along the load direction. The shear fracture has a smooth and symmetric feature. Such failure mode is commonly defined as tearout or shear-out failure in the publications [17–20,31,32].

2) A favorable ductile feature is found in the load-displacement curves of SD connections, as shown in Fig. 8. The load-displacement curve can be clearly divided into three stages. The first stage is an approximate linearly increasing stage where the applied load is proportional to the deformation. The second stage is a hardening stage where a clear nonlinear relationship is observed between the load and deformation. The third stage is a softening stage. The load drops with the increasing of deformation. The macro fractures present at the end of this stage, as shown in Fig. 7.

3) Compared to steel grade, end distance e_1 is a more significant factor influencing the bearing behavior of SD connection. A clear linear relationship is found between the normalized ultimate bearing resistance and e_1/d_0, as shown in Fig. 9. The normalized ultimate bearing resistance is the ratio of ultimate bearing resistance to $f_u dt$ where f_u is tensile stress, d is bolt diameter, t is plate

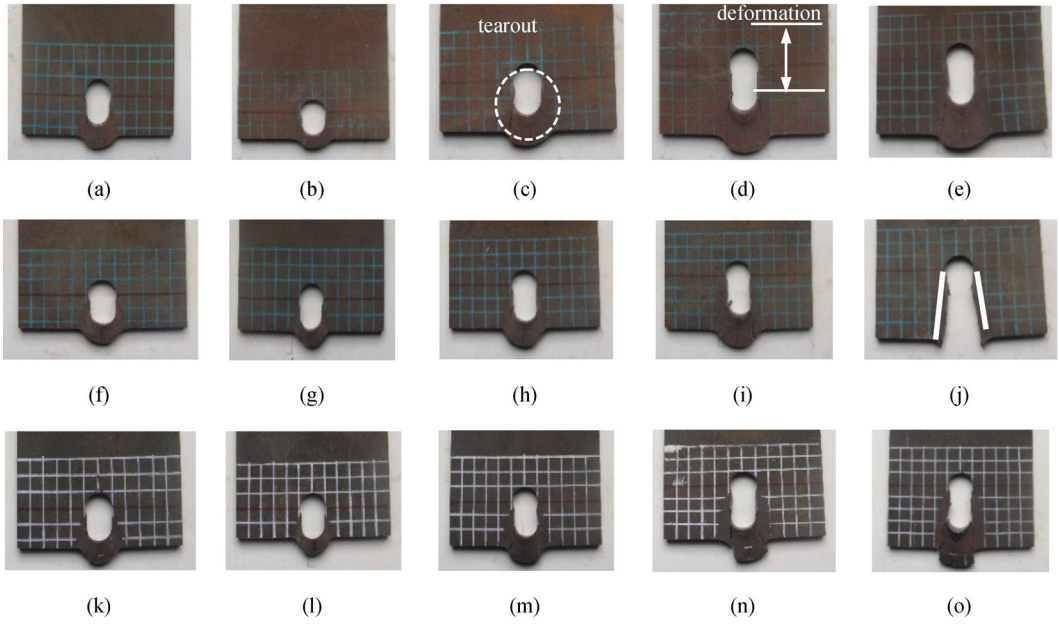

Fig. 7 Tearout failure mode of SD connection [32,33]. (a) SD-10-30-550; (b) SD-12-30-550; (c) SD-15-30-550; (d) SD-20-30-550; (e) SD-25-30-550; (f) SD-10-30-690; (g) SD-12-30-690; (h) SD-15-30-690; (i) SD-20-30-690; (j) SD-25-30-690; (k) SD-10-30-890; (l) SD-12-30-890; (m) SD-15-30-890; (n) SD-20-30-890; (o) SD-25-30-890. (Reprinted from Journal of Constructional Steel Research, 137, Wang Y B, Lyu Y F, Li G Q, Liew J Y R, Behavior of single bolt bearing on high strength steel plate, 19–30, Copyright 2017, with permission from Elsevier. Reprinted from Journal of Constructional Steel Research, 153, Lyu Y F, Wang Y B, Li G Q, Jiang J, Numerical analysis on the ultimate bearing resistance of single-bolt connection with high strength steels, 118–129, Copyright 2019, with permission from Elsevier.)

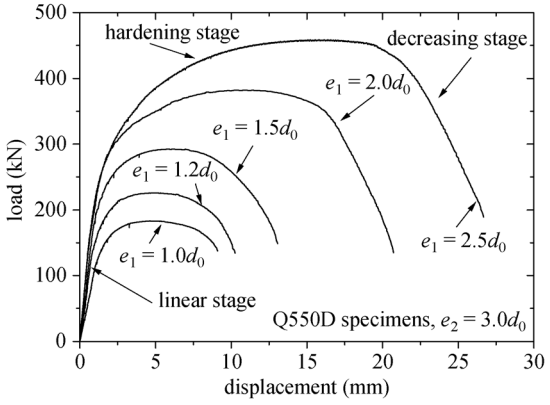

Fig. 8 Load-displacement of SD connections [32,33]. (Reprinted from Journal of Constructional Steel Research, 137, Wang Y B, Lyu Y F, Li G Q, Liew J Y R, Behavior of single bolt bearing on high strength steel plate, 19–30, Copyright 2017, with permission from Elsevier. Reprinted from Journal of Constructional Steel Research, 153, Lyu Y F, Wang Y B, Li G Q, Jiang J, Numerical analysis on the ultimate bearing resistance of single-bolt connection with high strength steels, 118–129, Copyright 2019, with permission from Elsevier.)

thickness. Meanwhile, the effect of end distance e_1 on the deformation capability of connection is significant. The corresponding deformation at the ultimate bearing resistance (denoted as D_u) for each SD connection is shown in Fig. 9(b). The D_u shows considerably increase with the parameter e_1/d_0. Up to 23% difference of D_u is observed for the specimens fabricated from different grades of steel. However, this 23% reduction does not contrary to the ductile feature of the curve.

4) A regression analysis based on least square methods is conducted with the test data shown in Fig. 9(a). Predicting formula Eq. (12) is established with R^2 of 0.98. The Eq. (12) reflects the relationship between the ultimate bearing resistance and parameter e_1/d_0. To verify the Eq. (12), extra 191 groups of results of single-bolt connections from the background documents of Eurocode3 [6–8] and related papers [17,19] were introduced, as shown in Fig. 10. The comparison shows that Eq. (12) is reasonably accurate to predict the ultimate bearing resistance of single-bolt connection. The R^2 drops from 0.98 to 0.93, which may be caused by material variability and unintended introduction of friction in the experiments.

$$F_{u,0} = 1.04\frac{e_1}{d_0}f_u dt. \tag{12}$$

3 Two-bolt connection in parallel

3.1 Previous findings

Puthli and Fleischer [13] observed three typical failure modes in the connection with two bolts positioned perpendicular to load direction. The first failure mode occurred when the edge distance e_2 and bolt spacing p_2 (defined in Fig. 1(b), p_2: bolt spacing, from center of bolt hole to center of nearby bolt hole perpendicular to load direction) was sufficient to avoid net cross-section failure while the end distance e_1 was comparatively small. This failure mode was the plate shear failure in the two-bolt connection as the cracks and bolt hole deformation were similar to the plate shear failure in single-bolt connections. The second failure mode was net cross-section failure. It was observed when edge distance e_2 and bolt spacing p_2 were both small compared to the end distance e_1. Necking phenomenon was found cross the whole net cross-section. The third failure mode was the block shear failure, which was referred as "mixed failure" by Puthli and Fleischer [13]. This type of failure occurred when edge distance e_2 was extremely smaller or larger than bolt spacing p_2. The

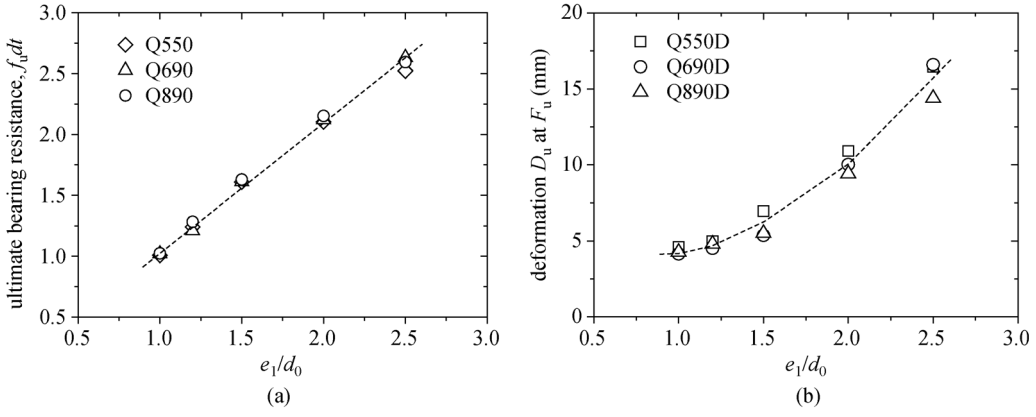

Fig. 9 Effect of end distance e_1 [32,33]. (a) Ultimate bearing resistance; (b) deformation at F_u. (Reprinted from Journal of Constructional Steel Research, 137, Wang Y B, Lyu Y F, Li G Q, Liew J Y R, Behavior of single bolt bearing on high strength steel plate, 19–30, Copyright 2017, with permission from Elsevier. Reprinted from Journal of Constructional Steel Research, 153, Lyu Y F, Wang Y B, Li G Q, Jiang J, Numerical analysis on the ultimate bearing resistance of single-bolt connection with high strength steels, 118–129, Copyright 2019, with permission from Elsevier.)

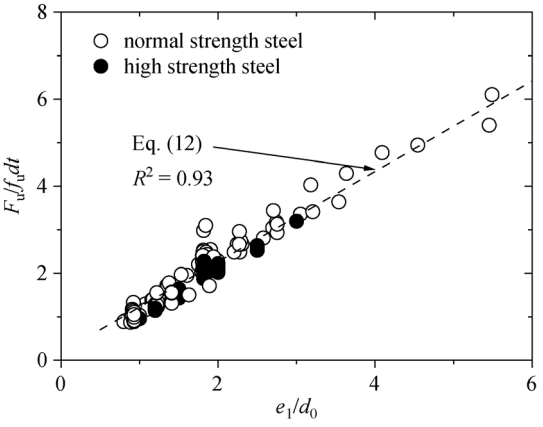

Fig. 10 Comparison with extra experimental results [32,33]. (Reprinted from Journal of Constructional Steel Research, 137, Wang Y B, Lyu Y F, Li G Q, Liew J Y R, Behavior of single bolt bearing on high strength steel plate, 19–30, Copyright 2017, with permission from Elsevier. Reprinted from Journal of Constructional Steel Research, 153, Lyu Y F, Wang Y B, Li G Q, Jiang J, Numerical analysis on the ultimate bearing resistance of single-bolt connection with high strength steels, 118–129, Copyright 2019, with permission from Elsevier.)

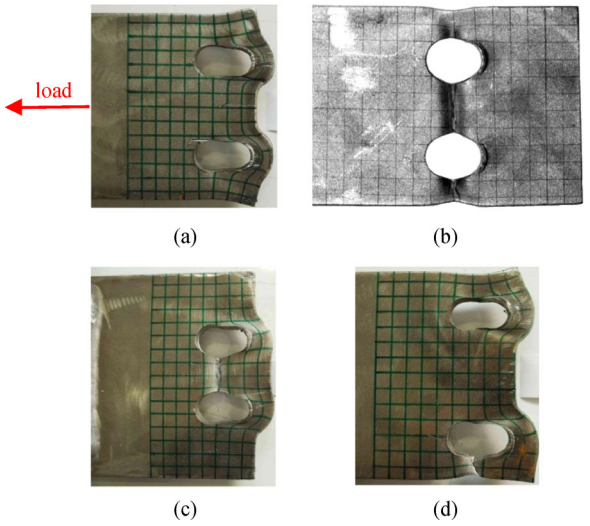

Fig. 11 Failure modes of two-bolt connection by Može and Beg [17,19]. (a) Plate shear failure; (b) net cross-section failure; (c) mixed failure I; (d) mixed failure II. (Reprinted from Journal of Constructional Steel Research, 66(8–9), Može P, Beg D, High strength steel tension splices with one or two bolts, 1000–1010, Copyright 2010, with permission from Elsevier. Reprinted from Journal of Constructional Steel Research, 95, Može P, Beg D, A complete study of bearing stress in single bolt connections, 126–140, Copyright 2014, with permission from Elsevier.)

mixed failure had two forms which were caused by insufficient edge distance e_2 or bolt spacing p_2. However, obvious elongation was observed no matter what form of the mixed failure occurred. The research aimed to check the minimum requirement on edge distance e_2 and bolt spacing p_2 specified by Eurocode3. They concluded that the minimum requirement in Eurocode3 was still applicable for HSS S460. In addition, they recommended an increase of design bearing resistance for connection with e_2 less than 1.5 times bolt hole diameter and p_2 less than 3.0 times bolt hole diameter.

Može and Beg [17,19] conducted a series of test of the two-bolt connections fabricated from conventional steel S235 and HSS S690. The failure modes of plate shear, net cross-section failure and the two forms of mixed failure are shown in Fig. 11, which are similar to those observed by Puthli and Fleischer [13]. Može and Beg [19] in 2014 referred the mixed failure as block shear failure. The block shear check according to Eurocode3 and AISC 360-16 were attempted to predict the ultimate load of the mixed failure. It was found that the block shear check of Eurocode3 yielded very conservative results. Although better than Eurocode3, the AISC 360-16 prediction was 12% to 15% lower than the experimental resistance. Based on the test results, Može and Beg [17–19] concluded that the edge distance e_2 and bolt spacing p_2 had no significant influence on the bearing resistance of the two-bolt connection when block shear failure is prevented. The effect of edge distance e_2 and bolt spacing p_2 were recommended to be excluded from the calculation of bearing resistance of bolted-connections.

A more detailed research on the block shear failure was conducted by Teh and Uz [35–39]. Based on test observations, it was proposed by Teh and Uz that the effective shear failure planes were located between the net and gross shear planes, as shown in Fig. 12. As a result, a new formula Eq. (13), was proposed. Compared to current AISC 360-16 [27], Eq. (13) achieved a more reasonable prediction of block shear resistance.

$$F_{\text{block}} = A_{\text{nt}} f_{\text{u}} + 0.6 A_{\text{ev}} f_{\text{u}}, \tag{13}$$

where A_{nt} and A_{ev} are defined in Fig. 12.

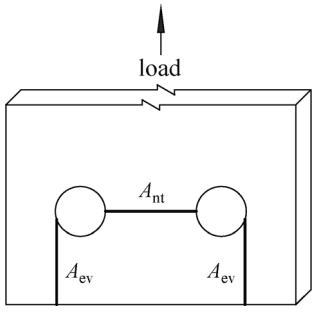

Fig. 12 Net tension failure planes (A_{nt}) and effective shear failure planes (A_{ev}).

3.2 Test results and findings at Tongji University

The convention of two-bolt connection perpendicular to load direction is denoted as TH-e_1/d_0-e_2/d_0-p_2/d_0-steel

grade. For TH connection, the end distance e_1 of $1.2d_0$ and $1.5d_0$ and the spacing distance p_2 of $2.7d_0$ and $3.5d_0$ are adopted in the test. The plate thickness is 10mm while d_0 = 26 mm.

The failure mode observed in the TH connection is shown in Fig. 13. Due to similarity of different steel grades, only the test results of the Q550D specimens are presented. For the specimens with different geometries, two failures mode are observed. For TH-15-20-27 with e_1/e_2 = 0.75, negligible rotation of net cross-section is observed. For TH-15-15-35 with e_1/e_2 = 1.0, rotation of net cross-section is found, as shown in Fig. 13. The rotation of net cross-section is caused by inadequate edge distance e_2. Despite the rotation of net cross-section occurs, the similar shear fracture is found in all the TH connections whether the rotation of net cross-section exists or not.

The load-displacement curves of the Q550D specimens are shown in Fig. 14. The three stages observed in the single-bolt connection can be clearly distinguished in Fig. 14. Compared to the single-bolt connection, the effect of e_1 on the load-displacement curve is similar. The comparison of D_u between TH connection and SD connection is conducted in Table 4. Under the condition of same end distance e_1 and steel grade, D_u of TH connection is found similar to the result of SD connection. The maximum difference is within 10%. Such result indicates that the two bolts in parallel transfers the load almost independently.

The ultimate bearing resistance of each TH connection is shown in Table 5. For each TH connection, result of SD connection with the same e_1 is also listed. It is found that ultimate bearing resistance of TH connection is 95%–105% of the doubled result of SD connection. This phenomenon confirmed that an individual bolt in TH connection can be treated as an equivalent SD connection. Ultimate bearing resistance of TH connection can be calculated by the sum of two SD connections with the same e_1.

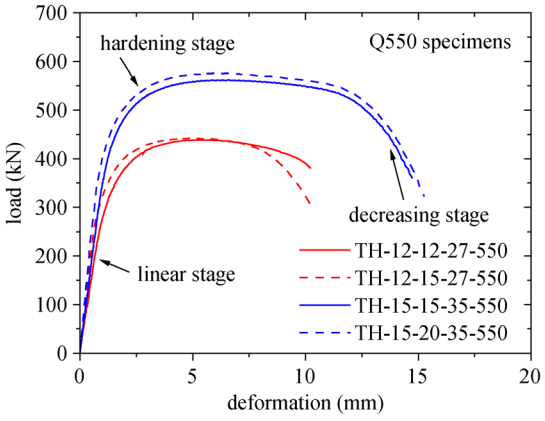

Fig. 14 Load-displacement curve of TH connections.

Table 4 D_u of TH connections and comparison with SD connection

specimen	Q550D (mm)	Q690D (mm)	Q890D (mm)
TH-12-12-27	5.26	4.57	4.61
TH-12-15-27	5.29	4.46	4.61
SD-12-30	5.00	4.52	4.81
TH-15-15-35	6.64	5.52	5.54
TH-15-20-35	6.44	5.38	5.79
SD-15-30	6.96	5.37	5.52

Table 5 Ultimate bearing resistance of TH connections

specimen	Q550D (kN)	Q690D (kN)	Q890D (kN)
TH-12-12-27	439	516	620
TH-12-15-27	442	523	643
SD-12-30 (double)	452	498	656
TH-15-15-35	562	646	794
TH-15-20-35	576	654	834
SD-15-30 (double)	584	664	832

4 Two and multi-bolt connection in tandem

4.1 Previous findings

Frank and Yura [5] tested the connections with two bolts positioned parallel to load direction. Four typical failure modes were observed during the tests. The first was net cross-section failure. The second was bearing failure, which was observed in the specimens with large end distance e_1 and small bolt spacing p_1 (defined in Fig. 1(c), p_1: bolt spacing, from center of bolt hole to center of

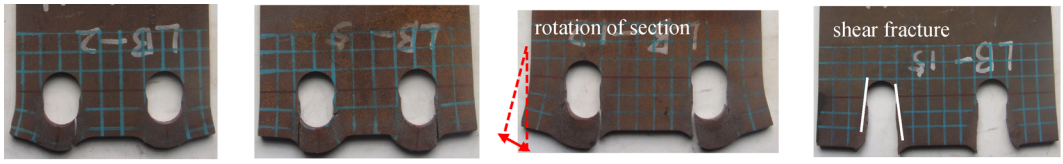

Fig. 13 Failure mode of TH connection [40]. (a) TH-12-12-27-550; (b) TH-12-15-27-550; (c) TH-15-15-35-550; (d) TH-15-20-35-550. (Reprinted from Journal of Constructional Steel Research, 155, Wang Y B, Lyu Y F, Li G Q, Liew J Y R, Bearing-strength of high strength steel plates in two-bolt connections, 205–218, Copyright 2019, with permission from Elsevier.)

nearby bolt hole parallel to load direction). The name of "bearing failure" was proposed by Frank and Yura [5] due to the excessive bolt hole elongation under bearing action. Different deformation patterns between the net cross-section failure and bearing failure were found. The net cross-section failure was characterized by a uniform grid distortion while a localized distortion of grid was found in bearing failure. The third failure mode was plate buckling. This failure mode occurred due to insufficient lateral restraint. The fourth failure mode was the end tearout failure which was observed in the specimens with small end distance e_1 and comparatively large bolt spacing p_1. They found that the load-displacement curve of the specimen with long end distance e_1 was essentially identical to those with short end distance e_1 when the bolt spacing p_1 was same, except for the initial stiffness. The specimen with short end distance e_1 was not as stiff as that with long end distance e_1. Accordingly, long end distance e_1 is recommended by Frank and Yura [5] in the design of bearing-type connection due to larger connection stiffness.

The deformation of 6.35 mm was first proposed by Frank and Yura [5] to consider the excessive hole elongation in bearing-type connection. This deformation limits originated in the research on the splice connections with undeveloped fillers. An important concept as the maximum useful loads was proposed to define the load at a specified deformation. It was observed in the research by Perry [41] that a deformation of 6.35 mm rendered most of the tested splice plates useless due to the extensive buckling. Approximate 80 percent of the ultimate load was already achieved at the deformation of 6.35 mm while an additional deformation of 19 mm was required to develop the rest of the resistance. As a result, the load at 6.35 mm deformation was suggested as the limit. Frank and Yura [5] accepted this suggestion and tested this deformation limit with load-displacement curves from Winter [42], Chang and Matlock [43], de Back and de Jona [44], and Munse [45]. It was found that bearing-type connections have very little resistance increase after 6.35 mm. Thus, a connection deformation limit of 6.35 mm was recommended as a limit state used on bearing capacity.

Aalberg and Larsen [14,15] tested several two-bolt connections with two bolts positioned parallel to load direction. Net cross-section failure and plate buckling were prevented in the design of test. It was found that the failure mode of the specimens fabricated from three grades of steel was similar, as well as the deformation capacity. The deformation at ultimate resistance for the specimen with a yield stress of 830 MPa had no significant difference compared with the specimen with a yield stress of 388 MPa. For the specimen with a yield stress of 1340 MPa, an up to 30% reduction was found. The failure mode of single-bolt connection was compared with the failure mode of two-bolt connection. It was observed that similar fracture profile could be observed between the two different types of connection. This indicated a similar load-carrying behavior for an individual bolt in two different types of connection.

Može and Beg [18] provided the test results of three-bolt and four-bolt connections. Four failure modes were observed, as shown in Fig. 15. The shear fracture was found in the first and the second failure modes. For the first failure mode (see Fig. 15(a)), the end distance e_1 was smaller than the bolt spacing p_1. The final failure was similar to the splitting failure of single-bolt connections. The second failure mode (see Fig. 15(b)) was found in the specimen with large end distance e_1 and comparatively small bolt spacing p_1. The final shear fracture was

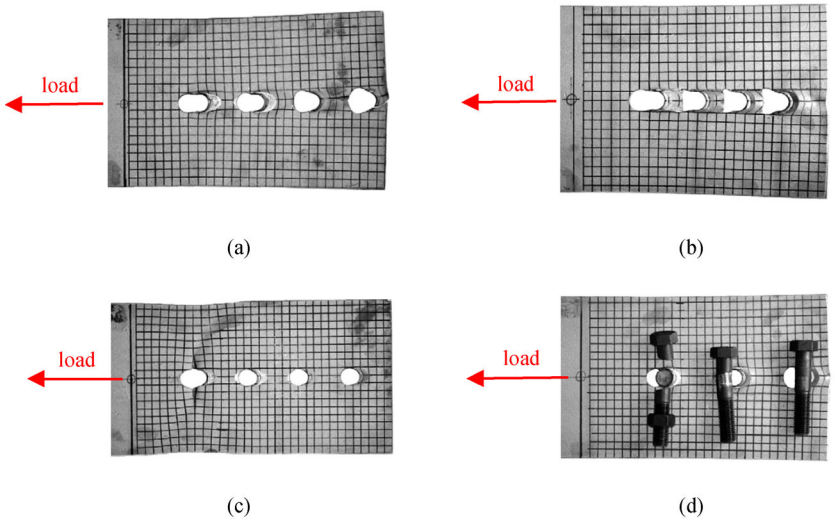

Fig. 15 Failure mode of multi-bolt by Može and Beg [18]. (a) Splitting failure; (b) failure between bolts; (c) net cross-section failure; (d) bolt shear failure. (Reprinted from Journal of Constructional Steel Research, 67(3), Može P, Beg D, Investigation of high strength steel connections with several bolts in double shear, 333–347, Copyright 2011, with permission from Elsevier.)

observed between bolts parallel to the load direction. The third failure mode (see Fig. 15(c)) was the net cross-section failure which was due to the insufficient edge distance e_2. The fourth failure mode (see Fig. 15(d)) was bolt shear failure. Although grade 12.9 high strength bolts were used in the test, bolt shear failure was not avoided. This was caused by the increased steel strength, which made the bolt shear as critical issue in design. An intended shift of bolt hole position by 2 mm was imposed to one bolt so that only one bolt was activated to transfer the load for the initial 2 mm deformation, as shown in Fig. 16. This measure was designed by Može and Beg [18] to determine the local ductility of HSS (S690). It was found that HSS had sufficient local ductility to redistribute the load. The imposed 2 mm shift of bolt hole had negligible effect on the ultimate resistance. With the assistance of numerical simulation, the distributed load on each bolt was also determined. Two distribution patterns were discovered. The first failure mode (see Fig. 15(a)) showed a non-uniform distribution of the bearing load on each bolt. The second failure (see Fig. 15(b)) and net cross-section failure showed an uniform distribution of the bearing load among bolts.

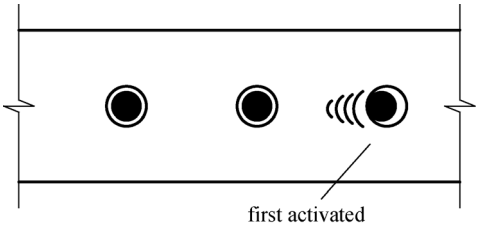

Fig. 16 First activation of one bolt.

Teh and Uz [46] conducted a comprehension study on the ultimate resistance of multi-bolt connection. It was found that the practical governing limit state for two-bolt connections and multi-bolt connection designed by current AISC 360-16 [27] is more likely a combined bearing and shear-out, which is shown in Fig. 17. They pointed out that the ultimate load capacity of a multi-bolt connection failing in combined bearing and shear-out cannot be predicted by the simple summation of the respective ultimate bearing resistance and ultimate shear-out resistance, which is implicitly permitted in the existing design codes. As a result, Eq. (14) was proposed to predict the ultimate resistance of multi-bolt connections. Equation (14) achieved a more accurate prediction than the simple summation of the shear-out and bearing resistances.

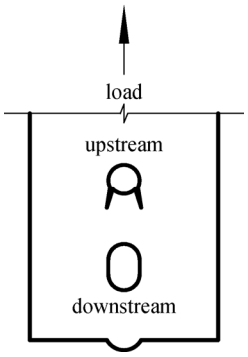

Fig. 17 Combined tearout and bearing in multi-bolt connection.

$$F_{\mathrm{bs}} = \left[\frac{e^2}{2.5d} + (n_{\mathrm{b}} - 1)3.5d\right] f_{\mathrm{u}} t, \tag{14}$$

where $e = e_1 - 0.25d_0$, d_0 is bolt hole diameter, n_{b} is total number of bolts in bolt line.

4.2 Test results and findings at Tongji University

The conventions for two-bolt and three-bolt connections in tandem are denoted as TV-e_1/d_0-e_2/d_0-p_1/d_0-steel grade and TP-e_1/d_0-e_2/d_0-p_1/d_0-steel grade, respectively. For TV connection, the end distance e_2 is fixed as $4.5d_0$ to avoid failure on the net cross-section. Four values of e_1/p_1 including 0.66, 1.0, 1.25, and 1.5 are designed. Compared to TV connection, one more bolt is designed in the TP specimens. The bolt end distance e_2 is also fixed as $4.5d_0$. Three values of e_1/p_1 including 0.66, 1.25, and 1.50 are designed. The plate thickness is 10 mm while $d_0 = 26$ mm.

The failure mode found in the TV connection (Q550D results) is shown in Fig. 18. The effect of steel grades is negligible on the profile of failure mode. The shear fracture along the load direction is observed in front of the two bolts. Plate deformation is localized around bolt hole, which is similar to SD connection and TH connection. Similar profile of failure can be observed in the TP connection, which is illustrated in Fig. 19. The obvious bolt elongation in the failure mode of TP connection

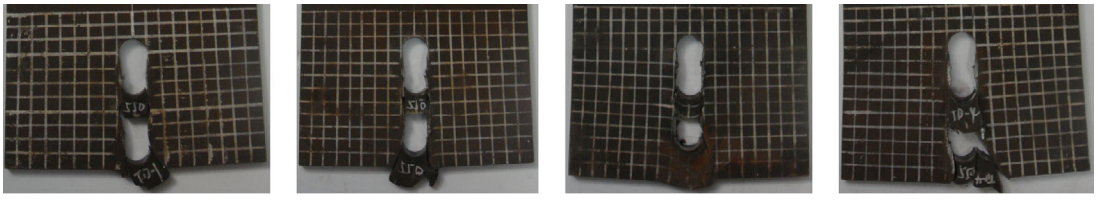

Fig. 18 Failure mode of TV connection. (a) TV-20-45-20-550; (b) TV-25-45-20-550; (c) TV-30-45-20-550; (d) TV-20-45-30-550.

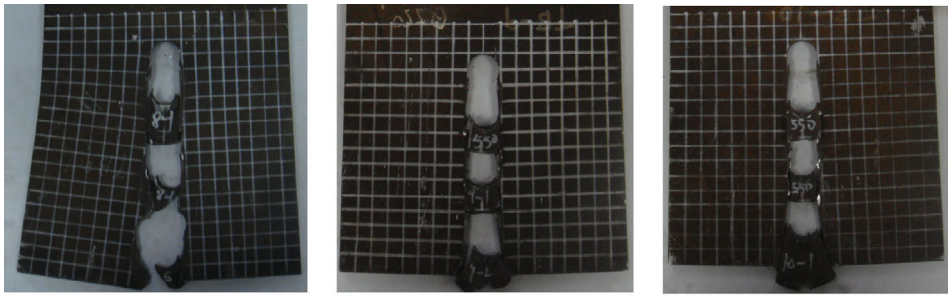

(a) (b) (c)

Fig. 19 Failure mode of TP connection. (a) TP-20-45-30-550; (b) TP-25-45-20-550; (c) TP-30-45-20-550.

indicates a ductile behavior of a group of fasteners.

The load-displacement curves of TV and TP connections (Q550D) are shown in Fig. 20. The shape of the load-displacement in TV and TP is similar to that of the SD and TH connections. Although different ($e_1 + p_1$) and ($e_1 + 2p_1$) are set for TV and TP connections, the deformation capability of different specimens shows no significant difference, as shown in Fig. 20. For convenient description, the bolt near plate edge in TV or TP connection is defined as end bolt and other bolts are defined as inner bolts. The D_u of SD-20-30 series is compared with TV and TP connections, as shown in Fig. 20. The results of SD-20-30 series are chosen since the value of e_1 and p_1 is $2.0d_0$ for all the TV and TP connection. For TV-20-45-30 and TP-20-45-30 series with $e_1 = 2.0d_0$, the load-displacement curve levels off at the D_u of SD-20-30. The subsequent increase in the resistance of the whole connection is negligible. The underlying reason for this phenomenon is that the end bolt has reached the ultimate bearing resistance. Behavior of the end bolt enters into the decreasing stage. As a result, the overall behavior of the whole connection shows a plateau branch. It is also found that, at the D_u, the behavior of SD-20-30 for TV and TP connections with $p_1 = 2.0d_0$ is similar to the single-bolt connection with $e_1 = 2.0d_0$. Such similarity indicates that the inner bolt with $p_1 = 2.0d_0$ has a similar deformation capability to the end bolt with $e_1 = 2.0d_0$.

The ultimate bearing resistances of TV and TP connections are summarized in Table 6. The effect of steel grade on the normalized ultimate bearing resistance is negligible in the TV and TP connections. It can be found from Table 6 that the specimens with larger ($e_1 + p_1$) or ($e_1 + 2p_1$) show higher resistance. For TV-20-45-20-550 and TV-30-45-20-550, an increase of ($e_1 + p_1$) by $1.0d_0$ results in the increase in the ultimate bearing resistance of 142 kN. This phenomenon indicates that the increasing of e_1 and p_1 is an effective strategy to achieve improved connection resistance. Due to limitation of experimental measurement method, actual load distributed on each bolt of TV and TP connections cannot be directly extracted from the experiments. Further numerical analysis is necessary.

5 Comparison with design codes

5.1 Brief introduction of existing codes

5.1.1 Eurocode3

The design bearing resistance of individual fastener in Eurocode3 is calculated by Eq. (15). As introduced in

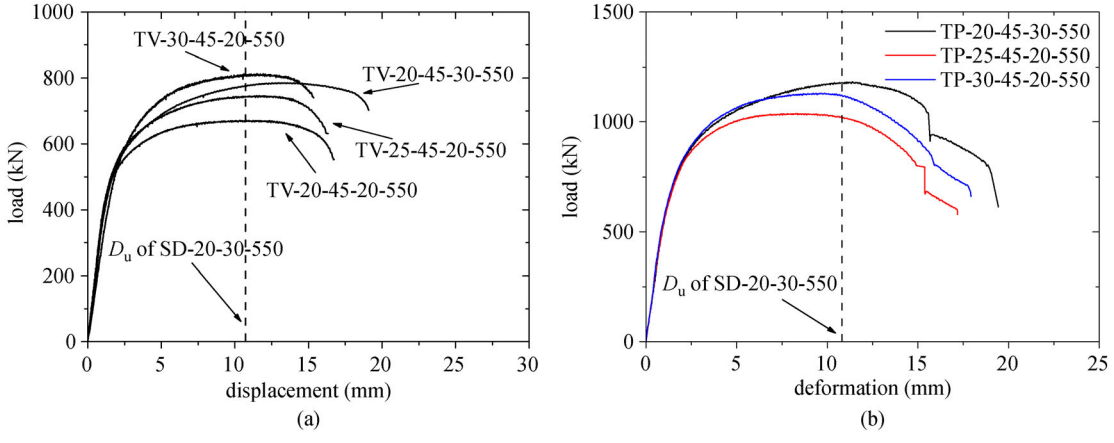

Fig. 20 Load-displacement of TV and TP connections. (a) TV specimens; (b) TP specimens.

Table 6 Ultimate bearing resistance of TV and TP connections

specimen	Q550D (kN)	norm*	Q690D (kN)	norm	Q890D (kN)	norm
TV-20-45-20	671	3.69	766	3.64	961	3.65
TV-25-45-20	746	4.11	850	4.04	1062	4.04
TV-30-45-20	813	4.48	932	4.43	1151	4.37
TV-20-45-30	785	4.32	895	4.26	1115	4.24
TP-20-45-30	1178	6.48	1364	6.49	1648	6.27
TP-25-45-20	1031	5.67	1174	5.58	1502	5.71
TP-30-45-20	1124	6.19	1279	6.08	1623	6.17

*Note: The normalized ultimate bearing resistance.

Section 2.1, two parts as $\alpha_b k_1 f_u dt$ and $2.5 f_u dt$ in Eq. (15) are set for different conditions. The first part $\alpha_b k_1 f_u dt$ is aimed to exclude the tearout failure while the second part $2.5 f_u dt$ is aimed to limit bolt hole elongation. The parameter α_b is set to consider effect of geometry parallel to load direction (e.g., end distance e_1) while the parameter k_1 is set to consider the effect of geometry perpendicular to load direction (e.g., edge distance e_2).

$$F_{b,EC3} = \alpha_b k_1 f_u dt \leqslant 2.5 f_u dt, \tag{15}$$

where $F_{b,EC3}$ is design bearing resistance of Eurocode3, α_b and k_1 are calculated according to end distance e_1 and edge distance e_2 as follows.

$$\text{For edge bolts, } \alpha_b = \min\left(\frac{e_1}{3d_0};\ \frac{f_{ub}}{f_u};\ 1\right), \tag{15a}$$

$$k_1 = \min\left(2.8\frac{e_2}{d_0} - 1.7;\ 2.5\right), \tag{15b}$$

$$\text{For inner bolts, } \alpha_b = \min\left(\frac{p_1}{3d_0} - \frac{1}{4};\ \frac{f_{ub}}{f_u}; 1\right), \tag{15c}$$

$$k_1 = \min\left(1.4\frac{p_2}{d_0} - 1.7; 2.5\right), \tag{15d}$$

where f_{ub} is the ultimate tensile strength of bolt.

5.1.2 AISC 360-16

The bearing resistance formulae in current AISC 360-16 are shown in Eq. (16). Clear distance denoted as l_c is used in AISC 360-16. Unlike Eurocode3, AISC 360-16 set two cases according to whether deformation around bolt hole is a design consideration at service load.

1) When the deformation around bolt hole is not a design consideration at service load, the bearing strength at bolt hole is calculated as:

$$F_{b,AISC} = \min(F_{tearout}, F_{bearing}), \tag{16a}$$

$$\text{Tearout: } F_{tearout} = 1.5 l_c t f_u, \tag{16b}$$

$$\text{Bearing: } F_{bearing} = 3.0 f_u dt. \tag{16c}$$

2) When the deformation around bolt hole is a design consideration at service load:

$$F_{b,AISC} = \min(1.2 l_c t f_u,\ 2.4 f_u dt), \tag{16d}$$

$$\text{Tearout: } F_{tearout} = 1.2 l_c t f_u, \tag{16e}$$

$$\text{Bearing: } F_{bearing} = 2.4 f_u dt, \tag{16f}$$

where $F_{b,AISC}$ is design bearing resistance of AISC 360-16, l_c is the clear distance in the direction of the force, between the edge of the hole and the edge of the adjacent hole or edge of the material, $F_{b,AISC}$ is design bearing resistance of AISC 360-16.

5.1.3 Chinese code GB50017-2017

The bearing resistance formula in current Chinese code GB50017-2017 is shown in Eq. (17). A parameter named as bearing strength f_c^b is used in Eq. (17). This parameter is related only to the tensile stress of steel. No effect of geometry (e.g., end distance e_1) is considered in the f_c^b, which show a different design methodology of Chinese code compared to current Eurocode3 and AISC 360-16.

$$F_{b,CH} = d \sum t \cdot f_c^b, \tag{17}$$

where $F_{b,CH}$ is design bearing resistance of Chinese code GB50017-2017, the parameter $f_c^b = 1.26 f_u$.

5.2 Comparisons

The above three codes are used to predict the bearing resistance of single-bolt connections. The measured geometric dimensions and material properties are used in the calculation while all partial factors were set as 1.0.

The comparison between the test results and the prediction by existing codes is shown in Fig. 21. For AISC 360-16, the Eq. (16a) is used to evaluate the ultimate bearing resistance of different connections. The prediction for the SD connection, TH connection, TV connection, and

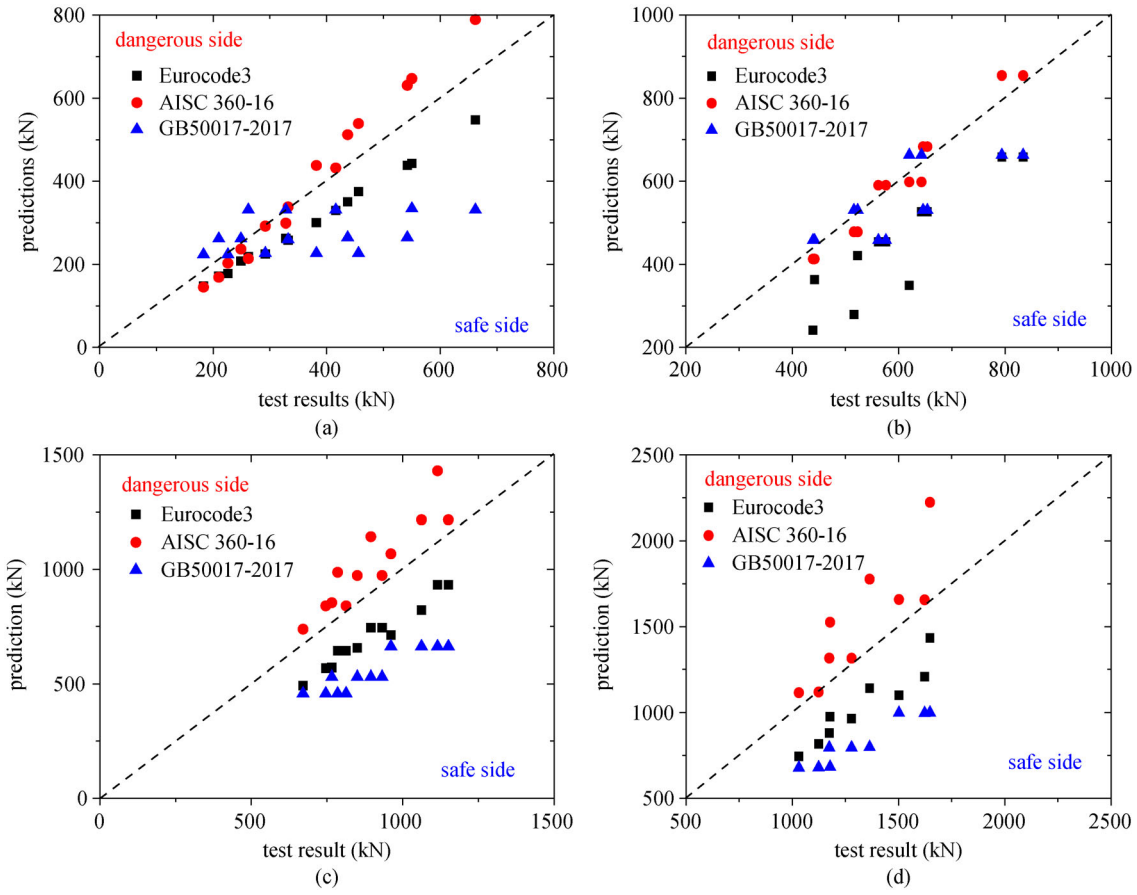

Fig. 21 Distribution of prediction for different connection types. (a) Single-bolt connection (SD); (b) two-bolt connection perpendicular to load direction (TH); (c) two-bolt connection parallel to load direction (TV); (d) three-bolt connection parallel to load direction (TP).

TP connection are shown in Figs. 21(a)–21(d), respectively. Evaluations are summarized in terms of connection types defined in Fig. 1.

1) Single-bolt connection (SD)

For Eurocode3, the predicted resistance lies on the safe side. The relative difference between the test result and prediction is from −16% to −23% according to end distance e_1. Similar conservative predictions can be found in the research by Može and Beg [17,19] as well as Aalberg and Larsen [14,15]. The research by D'Antimo et al. [47] on the bearing resistance in tubular structures also verifies such conservative prediction by Eurocode3.

For AISC 360-16, it is found that the safety margin of the prediction varies according to the value of end distance e_1. If $e_1 < 1.5d_0$, the predicted resistance by AISC 360-16 is lower than the test result. These data are distributed on the safe side. For specimen with $e_1 = 1.5d_0$, the prediction by AISC 360-16 agrees very well with the test result. The relative difference is within ±5% for different grades of steel. If $e_1 > 1.5d_0$, the AISC 360-16 provides unsafe prediction. The largest difference is observed close to + 20%.

For Chinese code GB50017-2007, it is found that the predicted resistance has excellent agreement with the test result when e_1 is around $1.2d_0$. For $e_1 < 1.2d_0$, prediction by GB50017-2007 is unsafe. For $e_1 > 1.2d_0$, prediction by GB0017-2007 is far more conservative than Eurocode3. The largest difference is up to −50%. According to the GB50017-2007, the minimum requirement of e_1 is $2.0d_0$. Thus, the prediction by GB0017-2007 is conservative for practical design.

2) Two-bolt connection perpendicular to load direction (TH)

For Eurocode3, two typical distributions of data are found, as shown in Fig. 21(b). One is the distribution with the relative difference close to −45% and the other is around −20%. The distribution with −45% difference is found in the series TH-12-12-27 with three grades of steel. Due to $e_2 = 1.2d_0$, the parameter k_1 for TH-12-12-27 in Eq. (4) equals 1.66. Compared to $e_2 = 1.5d_0$ (e.g, TH-12-15-27), an extra reduction of 34% is introduced for the series TH-12-12-27. The parameter k_1 in Eurocode3 considers the effect of edge distance e_2 on the resistance. However, such reduction is unnecessary because the predicted resistance is already lower than the test result by about −20%. Thus, it is recommended that the

parameter k_1 can be set constant as 2.5 for different values of edge distance e_2.

For AISC 360-16, the predicted resistance is lower than or close to the test result. For GB50017-2017, predicted resistance is close to the test result for TH connection with $e_1 = 1.2d_0$. For TH connection with $e_1 = 1.5d_0$, the difference is about –20%. For TH connection with $e_1 = 1.2d_0$ and $e_1 = 1.5d_0$, the difference between the prediction and the test result is close to the that of SD connection.

3) Two-bolt or three-bolt connection parallel to load direction (TV and TP)

For Eurocode3, the predicted resistance lies on the safe side, as shown in Figs. 21(c) and 21(d). The difference between the prediction and the test result is about –25%, which shows a stable feature compared to SD and TH connection.

For AISC 360-16, the predicted resistance lies on the unsafe side, as shown in Figs. 21(c) and 21(d). The largest difference is over + 25%. The unsafe prediction by AISC 360-16 is caused by the unsafe prediction in SD connection when $e_1 > 1.5d_0$. For TV and TP connections, the parameter e_1 and p_1 both exceed the $1.5d_0$. As a result, an unsafe prediction is provided by the AISC 360-16.

For GB50017-2007, the prediction is far more conservative than Eurocode3. The conservative prediction by GB50017-2007 can also be explained by the prediction of SD connections. For $e_1 \geqslant 2.0d_0$, prediction by GB50017-2007 is lower than the test result with relative difference close to –50%. For TV and TP connections with e_1 and p_1 higher than $2.0d_0$, very conservative predictions by GB50017-2007 can be expected.

4) Summary of the evaluation

Based on the above observations, the applicability of current codes to HSSs can be summed as follows. Eurocode3 and GB50017-2007 are applicable for the design of bearing-type bolted connections in HSSs. But potential resistance exists for both two codes, which can be further improved to make the design more economic and efficient. For AISC 360-16, the prediction is unsafe. An extra safety factor should be considered if the AISC 360-16 is used for the design of bearing-type bolted connections in HSSs.

6 Conclusions

This paper presents a review of previous research on the bearing-type bolted connections in HSS structures. Based on the experimental observations and the analysis of the test results, the following conclusions can be drawn:

1) Similar failure modes were observed for the specimens fabricated from different grades of steel. Difference in the profile of failure mode between conventional steel and HSS is negligible. The reduction of deformation capacity is observed for ultra-high strength steel. But the reduced ductility is still sufficient for the local deformation to redistribute load among bolts.

2) The load-displacement curves of the specimens in different connection types show a ductile behavior with three clearly distinguished stages including linear stage, hardening stage and decreasing stage. The reduced ductility of ultra-high strength steel ($f_y \geqslant 1000$ MPa) may lead an up to 23% reduction of deformation at the ultimate bearing resistance. But the ductile feature of load-displacement curves are observed for all specimens in different grades of steel. A linear relationship between the normalized ultimate bearing resistance and end distance is observed in the single-bolt connections. With a linear regressive analysis based on least square method, a new ultimate resistance formula of single bolt is proposed. The proposed formula has satisfactory agreement with the existing test data from publications.

3) The increase of steel grade, end distance and bolt spacing parallel to load direction can effectively improve the ultimate bearing resistance of bearing-type bolted connections. The normalized ultimate bearing resistance is an effective parameter to consider the effect of steel grade on bearing resistance.

4) Investigation on the applicability of existing codes is conducted. The resistance formula in Eurocode3 and Chinese code GB50017-2007 can be extended to the design of bearing-type bolted connections in HSSs. The American code AISC 360-16 cannot be directly used for the design of bearing-type bolted connections in HSSs. An extra safety factor should be considered for the AISC 360-16 when applied to HSSs.

Acknowledgements The authors would like to acknowledge the funding support by the National Natural Science Foundation of China (Grant No. 51408428).

References

1. Hai L T, Li G Q, Wang Y B, Sun F F, Jin H J. Experimental investigation on cyclic behavior of Q690D high strength steel H-section beam-columns about strong axis. Engineering Structures, 2019, 189: 157–173
2. Li G Q, Wang Y B, Chen S W. The art of application of high-strength steel structures for buildings in seismic zones. Advanced Steel Construction, 2015, 11(4): 492–506
3. Wang Y B, Li G Q, Chen S W, Sun F F. Experimental and numerical study on the behavior of axially compressed high strength steel columns with H-section. Engineering Structures, 2012, 43: 149–159
4. Willms R. High Strength Steel for Steel Constructions. Malmo: Nordic Steel Construction Conference-NSCC, 2009
5. Frank K H, Yura J A. An Experimental Study of Bolted Shear Connections. Report No. FHWA-RD-81–148. 1981
6. Snijder H H, Ungermann D, Stark J W B, Sedlacek G, Bijlaard F S K, Hemmert-Halswick A. Evaluation of test results on bolted connections in order to obtain strength functions and suitable model factors Part A: Results. Eurocode 3, Commission of the European

Communities. Brussels: TNO, 1988
7. Snijder H H, Ungermann D, Stark J W B, Sedlacek G, Bijlaard F S K, Hemmert-Halswick A. Evaluation of test results on bolted connections in order to obtain strength functions and suitable model factors Part B: Evaluations. Eurocode 3, Commission of the European Communities. Brussels: TNO, 1988
8. Snijder H H, Ungermann D, Stark J W B, Sedlacek G, Bijlaard F S K, Hemmert-Halswick A. Evaluation of test results on bolted connections in order to obtain strength functions and suitable model factors Part C: Test data. Eurocode 3, Commission of the European Communities. Brussels: TNO, 1988
9. Owens G W, Dowling P J, Algar R J. Bolted Connections, Bearing Stresses in Connections using Grade 8.8 Bolts. CESLIC Report BC3. 1976
10. Owens G W, Kridge G J. Bolted Connections, Bearing Stresses in Connections using Grade 8.8 Bolts in Punched Holes. CESLIC Report BC5. 1980
11. Owens G W, Hargreaves A C. Bolted Connections, Bearing Stresses in Connections using Grade 8.8 Bolts-Stage 2. CESLIC Report BC6. 1980
12. Kim H J, Yura J A. The effect of ultimate-to-yield ratio on the bearing strength of bolted connections. Journal of Constructional Steel Research, 1999, 49(3): 255–269
13. Puthli R, Fleischer O. Investigations on bolted connections for high strength steel members. Journal of Constructional Steel Research, 2001, 57(3): 313–326
14. Aalberg A, Larsen P K. Bearing strength of bolted connections in high strength steel. In: Nordic steel construction conference 2001-NSCC 2001: Proceedings. Helsinki: NSCC, 2001, 859–866
15. Aalberg A, Larsen P K. The effect of steel strength and ductility on bearing failure of bolted connections. In: Proceedings of the 3rd European Conference on Steel Structures. Coimbra, 2002, 869–878
16. Rex C O, Easterling W S. Behavior and modeling of a bolt bearing on a single plate. Journal of Structural Engineering, 2003, 129(6): 792–800
17. Može P, Beg D. High strength steel tension splices with one or two bolts. Journal of Constructional Steel Research, 2010, 66(8–9): 1000–1010
18. Može P, Beg D. Investigation of high strength steel connections with several bolts in double shear. Journal of Constructional Steel Research, 2011, 67(3): 333–347
19. Može P, Beg D. A complete study of bearing stress in single bolt connections. Journal of Constructional Steel Research, 2014, 95: 126–140
20. Može P. Bearing strength at bolt holes in connections with large end distance and bolt pitch. Journal of Constructional Steel Research, 2018, 147: 132–144
21. Draganić H, Dokšanović T, Markulak D. Investigation of bearing failure in steel single bolt lap connections. Journal of Constructional Steel Research, 2014, 98: 59–72
22. Guo H C, Huang Y H, Liu Y H, Liang G. Experimental study on bearing capacity of Q460 high-strength steel bolted connections. China Civil Engineering Journal, 2018, 51: 81–89 (in Chinese)
23. Shi Y J, Bin P, Gang S, Wang Y H. Experimental study on high strength steel-plate bolted connections under shear force. Industrial Construction, 2012, 42: 56–61 (in Chinese)
24. Liu Suli, Chen C X, Wei W H, Zhang H. Experimental research on the mechanical properties of high strength bolts with bearing type. Anhui architecture, 2013, 2: 211–212 (in Chinese)
25. Wu Y H, Zhang Z Y, Ji H G. Experimental study on the bearing strength of hole wall of high strength bolt connections. Steel Construction, 2015, 12: 28–31
26. EN 1993-1-8. Eurocode 3: Design of Steel Structures-Part 1–8: Design of Joints. Brussels: European Committee for Standardization, 2005
27. AISC. Specifications for Structural Steel Buildings. ANSI/AISC 360-16. Chicago: American Institute of Steel Construction, Inc., 2016
28. GB50017-2017. Code for design of steel structures. Beijing: China Architecture & Building Press, 2018 (in Chinese)
29. Latour M, Rizzano G, D'Antimo M, Demonceau J F, Jaspart J P, Armenante V. Bearing strength of shear connections for tubular structures: An analytical approach. Thin-walled Structures, 2018, 127: 180–199
30. Teh L H, Uz M E. Effect of loading direction on the bearing capacity of cold-reduced steel sheets. Journal of Structural Engineering, 2014, 140(12): 06014005
31. Teh L H, Uz M E. Ultimate shear-out capacities of structural-steel bolted connections. Journal of Structural Engineering, 2015, 141(6): 04014152
32. Wang Y B, Lyu Y F, Li G Q, Liew J Y R. Behavior of single bolt bearing on high strength steel plate. Journal of Constructional Steel Research, 2017, 137: 19–30
33. Lyu Y F, Wang Y B, Li G Q, Jiang J. Numerical analysis on the ultimate bearing resistance of single-bolt connection with high strength steels. Journal of Constructional Steel Research, 2019, 153: 118–129
34. National Standardization Technical Committees. GB/T 228-2002 Metallic Materials: Tensile Testing at Ambient Temperature. Beijing: China Standard Press, 2002 (in Chinese)
35. Teh L H, Uz M E. Block shear capacity of bolted connections in cold-reduced steel sheets. Journal of Structural Engineering, 2012, 138(4): 459–467
36. Teh L, Deierlein G. Effective shear plane model for tearout and block shear failure of bolted connections. Engineering Journal-American Institute of Steel Construction, 2017, 54(3): 181–194
37. Teh L H, Uz M E. Block shear failure planes of bolted connections—Direct experimental verifications. Journal of Constructional Steel Research, 2015, 111: 70–74
38. Elliott M D, Teh L H. Whitmore tension section and block shear. Journal of Structural Engineering, 2019, 145(2): 04018250
39. Elliott M D, Teh L H, Ahmed A. Behaviour and strength of bolted connections failing in shear. Journal of Constructional Steel Research, 2019, 153: 320–329
40. Wang Y B, Lyu Y F, Li G Q, Liew J Y R. Bearing-strength of high strength steel plates in two-bolt connections. Journal of Constructional Steel Research, 2019, 155: 205–218
41. Perry W C. Bearing Strength of Bolted Connections. Thesis for the Master's Degree. Austin: The University of Texas at Austin, 1981
42. Winter G. Tests on bolted connections in light gage steel. Journal of the Structural Division, 1956, 82: ST2
43. Chang K P, Matlock R B. Light gage steel bolted connections

without washers. Journal of the Structural Division, 1975, 181: ST7
44. de Back J, de Jona A. Measurements on Connections with H.S.F.G. Bolts, Particularly in View of the Permissible Arithmetical Bearing Stress (a condensed version of Reports 6-66-1 by J. H. A. Struik and 6-67-5 by S. Wittermans). Report 6–68–3. 1968
45. Munse W H. The Effect of Bearing Pressure on the Static Strength of Riveted Connections. Urbana: University of Illinois, 1959
46. Teh L H, Uz M E. Combined bearing and shear-out capacity of structural steel bolted connections. Journal of Structural Engineering, 2016, 142(11): 04016098
47. D'Antimo M, Demonceau J F, Jaspart J P, Latour M, Rizzano G. Experimental and theoretical analysis of shear bolted connections for tubular structures. Journal of Constructional Steel Research, 2017, 138: 264–282